Two types of primary mucinous ovarian tumors can be distinguished based on their origin

Simons, Michiel; Simmer, Femke; Bulten, Johan; Ligtenberg, Marjolijn J.; Hollema, Harry; van Vliet, Shannon; de Voer, Richarda M.; Kamping, Eveline J.; van Essen, Dirk F.; Ylstra, Bauke

Published in:
Modern Pathology

DOI:
10.1038/s41379-019-0401-y

Publication date:
2020

Modern Pathology (2020) 33:722–733
https://doi.org/10.1038/s41379-019-0401-y

ARTICLE

Two types of primary mucinous ovarian tumors can be distinguished based on their origin

Michiel Simons[1] · Femke Simmer[1] · Johan Bulten[1] · Marjolijn J. Ligtenberg[1,2] · Harry Hollema[3] · Shannon van Vliet[1] · Richarda M. de Voer[2] · Eveline J. Kamping[2] · Dirk F. van Essen[4] · Bauke Ylstra[4] · Lauren E. Schwartz[5] · Yihong Wang[6] · Leon F. Massuger[7] · Iris D. Nagtegaal[1] · Robert J. Kurman[8,9,10]

Received: 29 August 2019 / Revised: 7 October 2019 / Accepted: 7 October 2019 / Published online: 6 November 2019

Abstract

The origin of primary mucinous ovarian tumors is unknown. We explore the hypothesis that they originate from either Brenner tumors or teratomas and examine differences between the tumors that arise in these settings. A total of 104 Brenner tumor-associated mucinous tumors and 58 teratoma-associated mucinous tumors were analyzed. Immunohistochemistry for 21 antigens and fluorescence in situ hybridization for *ERBB2* and *MYC* were performed. Genome-wide copy number analysis and mutation analysis for 56 cancer-related genes was carried out on a subset of mucinous ovarian tumors and their complementary Brenner tumor or teratoma. Patients with teratoma-associated mucinous tumors were significantly younger than patients with Brenner tumor-associated mucinous tumors (43 vs. 61 years). During progression from cystadenoma to atypical proliferative mucinous (borderline) tumor to carcinoma expression of typical gastrointestinal markers was increased in both Brenner tumor-associated and teratoma-associated mucinous tumors. Brenner tumor-associated mucinous tumors showed more frequently calcifications and Walthard cell nests, rarely expressed SATB2 and showed more often co-deletion of *CDKN2A* and *MTAP*. Teratoma-associated mucinous tumors were characterized by mucinous stromal dissection, SATB2 expression and *RNF43* mutations. Other frequent mutations in both Brenner tumor-associated and teratoma-associated mucinous tumors were *TP53* and *KRAS* mutations. Based on identical mutations or copy number profiles clonal relationships were indicated in two mucinous tumors and their associated Brenner tumor. Teratomas and Brenner tumors give rise to different subtypes of mucinous ovarian tumors. Subsequent progression pathways are comparable since both Brenner tumor-associated and teratoma-associated mucinous tumors develop a gastrointestinal immunophenotype during progression and show early mutations in *KRAS* and *TP53*. Teratoma-associated mucinous tumors may more closely resemble true gastrointestinal tumors, indicated by their expression of SATB2 and the presence of *RNF43* mutations.

Introduction

Primary mucinous ovarian carcinomas are relatively infrequent tumors. They are most often low grade, indolent

Supplementary information The online version of this article (https://doi.org/10.1038/s41379-019-0401-y) contains supplementary material, which is available to authorized users.

✉ Michiel Simons
Michiel.Simons@radboudumc.nl

[1] Department of Pathology, Radboud University Medical Center, Nijmegen, The Netherlands

[2] Department of Human Genetics, Radboud University Medical Center, Nijmegen, The Netherlands

[3] Department of Pathology, University Medical Center Groningen, Groningen, The Netherlands

[4] Department of Pathology, VU University Medical Center, Amsterdam, The Netherlands

[5] Department of Pathology and Laboratory Medicine, Hospital of the University of Pennsylvania, Philadelphia, PA, USA

[6] Department of Pathology, Sir Run Run Shaw Hospital, Zhejiang University School of Medicine, Hangzhou, China

[7] Department of Obstetrics and Gynecology, Radboud University Medical Center, Nijmegen, The Netherlands

[8] Department of Pathology, Johns Hopkins Medical Institutions, Baltimore, MD, USA

[9] Department of Gynecology and Obstetrics, Johns Hopkins Medical Institutions, Baltimore, MD, USA

[10] Department of Oncology, Johns Hopkins Medical Institutions, Baltimore, MD, USA

carcinomas, although it has been shown that prognosis of patients with mucinous ovarian carcinomas is strongly stage dependent [1]. In the now widely accepted, dualistic model of ovarian carcinogenesis, they are considered type I tumors, developing through a well-defined cystadenoma—atypical proliferative mucinous (borderline) tumor—carcinoma sequence. Although the cell of origin of primary mucinous tumors of the ovary is unknown, a growing body of literature suggests Brenner tumors and teratomas as possible sources [2].

Brenner tumors are ovarian tumors consisting of nests of transitional epithelium. The presence of mucinous tumors within Brenner tumors has been described with a frequency up to 33% [3–5]. Seidman et al. found specific types of calcifications occurring in both mucinous and Brenner tumors and complementary size distributions [4]. Immunohistochemical studies have shown that both the mucinous and the Brenner components have a non-Müllerian phenotype generally lacking expression of PAX2 and PAX8, while GATA3 expression in both components may be suggestive of a common source [3]. More recently, origin of mucinous tumors in Brenner tumors has also been supported by clonality studies using microsatellite genotyping [6]. *MYC* amplification found in a number of Brenner tumors and associated mucinous tumors is also suggestive of a clonal relationship [7].

Teratomas are thought to arise from oocytes following duplication errors in meiosis [8, 9]. Since all three germ layers are potentially allowed to develop, any type of tissue can be present in these tumors. Mucinous neoplasms coinciding with teratomas are commonly noted and express gastrointestinal markers, incompatible with a Müllerian phenotype [10–12]. Molecular studies using microsatellites and short tandem repeats have indicated a clonal relationship between teratomas and associated mucinous tumors [13–15].

Little is known about specific genetic alterations in these tumors such as copy number alterations or mutations and their role in progression from mucinous cystadenomas into atypical proliferative tumors and ultimately carcinomas. Ryland et al. have shown *KRAS*, *TP53*, and *CDKN2A* mutations in both mucinous cystadenomas, atypical proliferative tumors and carcinomas, whereas *BRAF* and *NRAS* mutations occurred solely in atypical proliferative tumors and carcinomas. *ERBB2* amplification appears to be a late event, since no cystadenomas showed this [16]. MacKenzie et al. carried out next generation sequencing, finding comparable results with additionally *PIK3CA* mutations occurring in a number of atypical proliferative tumors and carcinomas [17].

The aim of this study was to examine a possible clonal relationship between mucinous ovarian tumors occurring with Brenner tumors or teratomas in the same ovary, based on morphological, immunophenotypical and molecular changes. The genome-wide copy number analysis and somatic gene panel analyses for this purpose also served to investigate the differences in the development of mucinous tumors arising from Brenner tumors and teratomas.

Materials and methods

Case selection

The nationwide network and registry of histo- and cytopathology in the Netherlands codes and saves pathology reports in the Netherlands from 1971 with nationwide coverage from 1991 [18].

A search for all patients with Brenner tumor-associated mucinous tumors and teratoma-associated mucinous tumors was performed in the National Pathology Database (registration number lzv1140A and B). For this main search, Brenner tumor-associated mucinous tumors and teratoma-associated mucinous tumors were defined as any type of mucinous ovarian tumor occurring with either any type of Brenner tumor or any type of teratoma in the same ovary. Other inclusion criteria were diagnosis on complete resection of the ovary from 2000 until 2014. Patients with any contralateral ovarian tumor other than a Brenner tumor or teratoma (either with or without a mucinous tumor) were excluded, as were patients with any other genital tract malignancy. Histories of ovarian and tubal tumors to rule out inclusion of recurrences and gastrointestinal tract tumors to rule out metastatic ovarian tumors were searched additionally. The archives of the Johns Hopkins Hospital were also searched for available cases.

Demographic, macroscopic and histologic features

Age, laterality, and size were extracted from pathology reports. Slides of a subset of cases could be requested from 12 collaborating hospitals and were reviewed. Diagnosis, distribution of Brenner nests and mucinous cysts (separate compartments or mixed), presence of mucinous metaplasia of Brenner nests, presence of mucinous stromal dissection and calcifications were recorded. If the Fallopian tube was resected, the presence of Walthard cell nests and transitional cell metaplasia, defined as occurring at the tubo-peritoneal junction, were recorded as well.

Additional database searches: comparison of tumor subtypes

For age comparison between ovarian tumor subtypes, a search for all ovarian tumors of endometrioid and clear cell histology from 2000 until 2010 and for all serous tumors in 2000, 2005, and 2010 was performed in the National Pathology Database (registration number lzv1140C). Of

serous cystadenomas, serous borderline tumors, serous adenocarcinomas, endometrioid adenocarcinomas and clear cell adenocarcinomas, 200 cases each were included. Mixed tumors, bilateral tumors with different subtypes or differentiation, recurrences, tumors of uncertain origin and patients with a history of other malignancies were excluded. Endometrioid tumors were included if histology of the uterus was available and negative for endometrial endometrioid adenocarcinoma. Patients with other malignancies of the internal genital tract were excluded.

Tissue micro-array construction

Of a subset of requested cases found through the main search in the National Pathology Database, tissue blocks containing formalin-fixed paraffin embedded tissue were requested and 2 mm cores were taken for construction of tissue micro-arrays using the 3DHistech TMA Grand Master (Sysmex, Switzerland). Two cores were taken from each mucinous component and two cores of each Brenner component. Tissue micro-arrays were used for immunohistochemical staining and fluorescent in situ hybridization (FISH).

Immunohistochemical staining and FISH

Slides were stained for CK7, CK20, CDx2, ER, PR, WT1, PAX8, MUC4, CEA-m, Ki-67, p53, OC125, HNF4α, SATB2, p16, GATA3, Her2/neu, MSH2, MSH6, MLH1, PMS2. FISH was carried out for *ERBB2* and *MYC*. Details are found in the Supplementary Methods.

Interpretation of staining

All stains were scored for both dominant intensity (0 = negative, 1 = weak, 2 = moderate, 3 = strong) and percentage of positive tumor cells unless indicated otherwise. These scores were multiplied and the scores of both tissue micro-array cores were averaged. A score 0–20 was considered negative, 21–100 weakly positive, 101–200 moderately positive and 201–300 strongly positive. For binary scoring, a score higher than 20 was considered positive. Mismatch repair protein staining was considered positive in case of any amount of at least weak nuclear staining. P53 was considered mutated in case of diffuse (>60%), strong staining or complete absence of staining and wild type in case of heterogeneous staining. Ki-67 was scored as percentage of positive cells. Her2/neu staining, *ERBB2* FISH and ultimate Her2/neu status were determined according to the 2013 ASCO/CAP guidelines for breast cancer [19]. *MYC* FISH was scored as amplified when ratio *MYC*/cep8 ≥2.0 or nonamplified when the ratio <2.0.

DNA isolation

Areas of interest were marked on HE-stained slides and tumor cell percentage was scored (see Table S6 for estimated tumor cell percentages). Five to eight 30-µm-thick sections were cut from formalin-fixed paraffin embedded material, depending on the absolute amount of selected tumor cells. At the end a 4-µm-thick slide was HE-stained for comparison of the tumor containing area. After the sections were mounted on glass slides, the area of interest was manually microdissected and put into a 1.5 mL Eppendorf tube. Depending on the amount of tissue, 100–200 µL of 5% Chelex-100 in TET lysis buffer was added. Of this amount, 10% of proteinase K (20 mg/mL) was added. Samples were incubated in thermomix (Thermomixer comfort, Eppendorf) for at least 16 h at 56 °C, 350 rounds per minute (rpm). When all tissue was dissolved, samples were incubated for exactly 10 min at 95 °C, 350 rpm and centrifuged for 10 min at room temperature, 14,000 rpm. The supernatant containing DNA was transferred to a second 1.5 mL Eppendorf tube, separating it from the Chelex-100 and coagulated paraffin. DNA concentrations were measured using Qubit dsDNA BR Kit (Thermofisher). DNA from normal tissue was isolated if available from the same or another tissue block.

Genome-wide DNA copy number analysis

Shallow genome-wide sequencing for copy number analysis was performed at The Tumor Genome Analysis Core, department of Pathology, VU Cancer Center Amsterdam. In short, library preparation was carried out, comprising fragmentation of DNA by sonication, repair of DNA ends, 3′ adenylation, adapter ligation and purification and PCR amplification of the fragments with adapters and again purification. The Illumina Next Generation Sequencing platform was used for shallow whole-genome sequencing. The shallow whole-genome sequencing data were analyzed using the Bioconductor package QDNAseq [20]. Reads per 100 kbp bin were counted to make a genome-wide profile. Correction for sequence mappability and GC content was carried out, as well as filtering of problematic genomic regions. A subset of normal samples was analyzed and profiles were used for dewaving tumor genome-wide copy number profiles using the R-package 'NoWaves' [21]. Details of this method are described elsewhere [20].

Next generation sequencing using single-molecule molecular inversion probes

Details of this method are extensively described elsewhere [22]. Samples were selected based on a tumor cell

percentage of at least 20%. For preparation of the single-molecule molecular inversion probe pool for targeted enrichment, molecular inversion probes were designed for 56 cancer related genes using the procedure described elsewhere [23] (see Table S1). The single-molecule molecular inversion probes were divided over two pools. The molecular ratio between gDNA and single-molecule molecular inversion probes was set to 1:800 for every individual single-molecule molecular inversion probe. Per sample, four PCRs were performed and the resulting PCR products were pooled. Per run 47 up to 77 libraries were sequenced, depending on the presence of normal tissue samples for which lower read depth was accepted.

Variant selection

The commercial analysis software SeqNext (Sequence Pilot, JSI medical systems, Ettenheim, Germany) was used for read mapping and variant calling. Settings for generating consensus reads and variant calling are described elsewhere [22]. During coverage calculations read pairs are counted as two reads. Minimal absolute coverage was set at ≥20 combined reads. Variants were only called if the variant percentage was ≥5% and ≥5 combined reads present showing the variant. Variants identified in normal samples were filtered from the matching tumor samples. Intronic variants (outside the canonical splice sites) and synonymous variants were discarded. Variants with at least a three-fold difference in the number of forward and reverse reads, and SNPs with a population allele frequency in ExAC [24] ≥0.01 were removed.

Remaining variants with at least ≥10% allele frequency ≥10 combined reads and detection in at least two molecular inversion probes targeting opposite strands were selected. Variants were excluded if SeqNext hinted at cytosine deamination and allele frequency or number of combined reads were <10% or <10%, respectively. If these were ≥10% or ≥ 10%, variants were manually curated, as were those with mutant allele frequency between 5% and 10%. Exclusion criteria during manual curation were the following (a) variants within homo-polymers; (b) variants within reads with many Ns; (c) variants only present directly at the start or end of reads and absent in the overlapping molecular inversion probe; (d) variants in poorly aligned reads or reads representing pseudogenes; (e) suspected cytosine deaminations.

Concerning clonality, loci of variants detected in either a mucinous tumor or Brenner tumor or teratoma, were specifically reassessed in the complementary tumor (i.e., the aligned reads were evaluated) and coverage of the specific locus was determined.

Coverage per unique region was calculated using the aligned reads based on the output tables from SeqNext.

Statistical analysis

For comparison of means of two populations, independent t-tests were used, for distributions in two or more populations, Pearson's Chi-squared test was used (IBM SPSS Statistics v20.0). The statistical programming language R was used for copy number data analyses. To test for clonality between tumor pairs the R-package 'Clonality' was used [25]. First, the chromosomes were split into p and q arms, and the dewaved, median-normalized log2-transformed read counts per 100 kbp bin were averaged into blocks of three consecutive markers. Subsequently, clonality analysis was performed. This methodology uses an algorithm to identify the most significant change in each chromosome arm, then calls gains or losses and looks at matching patterns of gains or losses for the matching sample pairs and sample combinations that are independent by default using a log likelihood ratio measure. A p-value of < 0.05 was considered significant. In addition, the dewaved, median-normalized log2-transformed read counts per 100 kbp bin were segmented using R-package 'DNA-copy' [26] to determine the Pearson correlation between samples.

To identify differences in copy number alterations between Brenner tumor-associated and teratoma-associated mucinous tumor samples, these were called into five categories (deletion, loss, normal, gain or amplification) with the R-package 'CGHcall' [27] and a dimension reduction was performed with the R-package 'CGHregions' [28]. Subsequently, the Wilcoxon rank-sum test was performed for each chromosomal sub-region. A p-value of < 0.05 was considered significant.

Results

Age in relation to Brenner tumor-associated and teratoma-associated mucinous tumors

The main search identified 531 cases, of which 516 through the National Pathology Database and 15 through the Johns Hopkins Hospital. Of these, 352 were Brenner tumor-associated mucinous tumors, 178 were teratoma-associated mucinous tumors and one case had both a Brenner tumor and teratoma with a mucinous cystadenoma in one ovary. Mean age of all patients was 55 years. Mean age of patients with Brenner tumor-associated mucinous tumors was 61 and of patients with teratoma-associated mucinous tumors 43 years ($p < 0.001$), for carcinomas only, this was 60 and 62 years ($p = 0.84$).

Patients with Brenner tumor-associated mucinous tumors showed no age difference with patients with endometrioid ($p = 0.25$) and serous adenocarcinomas ($p = 0.85$). They

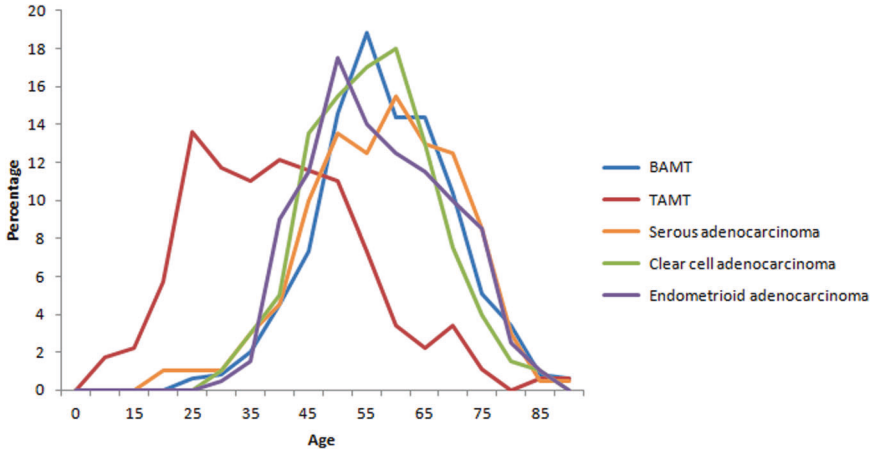

Fig. 1 Age distribution of patients with endometrioid, serous and clear cell adenocarcinomas and Brenner tumor-associated mucinous tumors and teratoma-associated mucinous tumors

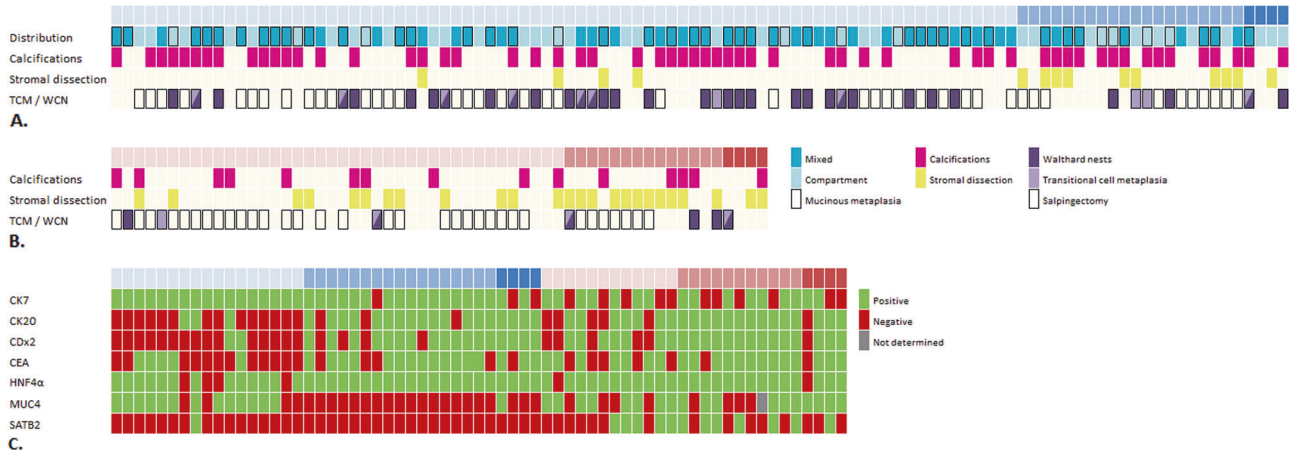

Fig. 2 a, **b** Differences in frequencies of histological characteristics and protein expression patterns in Brenner tumor-associated and teratoma-associated mucinous tumors, respectively. **c** Differences in frequencies of histological characteristics and protein expression patterns in Brenner tumor-associated and teratoma-associated mucinous tumors. Brenner tumor-associated mucinous tumors are indicated in blue, teratoma-associated mucinous tumors in red from light to dark for cystadenomas, atypical proliferative mucinous (borderline) tumors and carcinomas, respectively

were older than patients with clear cell carcinomas (mean age 59 years, $p = 0.02$) and patients with all serous tumors together (mean age 56 years, $p < 0.01$). Patients with teratoma-associated mucinous tumors were younger compared to patients with endometrioid (60 years, $p < 0.01$), clear cell (59 years, $p < 0.01$) and serous adenocarcinomas (61 years, $p < 0.01$) and all types of serous tumors together (56 years, $p < 0.01$) (Fig. 1 and Table S2).

Histology of Brenner tumor-associated and teratoma-associated mucinous tumors

Revised cases included 104 Brenner tumor-associated mucinous tumors (80 cystadenomas, 20 atypical proliferative tumors, and 4 carcinomas) and 58 teratoma-associated mucinous tumors (40 cystadenomas, 14 atypical proliferative tumors and 4 carcinomas) (Fig. 2a, b). One case (1%) was excluded after alteration of the diagnosis to serous cystadenoma, in 14 cases (9%) diagnosis was alters in means of cystadenoma, atypical proliferative tumor or carcinoma. Mean size, tumor laterality and frequency of salpingectomy did not differ significantly between the two groups. In case of Brenner tumor-associated mucinous tumors only, mucinous metaplasia was seen significantly more often in cases with mixed distribution of Brenner nests and mucinous cysts than in cases with compartmental distribution (63% vs. 25%, $p < 0.01$, Fig. 3a–c). Calcifications were significantly more often seen in Brenner tumor-associated mucinous tumors than in teratoma-associated mucinous tumors (56% vs. 22%, $p < 0.01$, Fig. 3d). Mucinous stromal dissection was significantly more often seen in teratoma-associated mucinous tumors (13% vs. 43%, $p < 0.01$, Fig. 2e). When the Fallopian tube was available for review, tubal Walthard cell nests were seen more often in Brenner tumor-associated mucinous tumors than teratoma-associated mucinous tumors (42% vs. 15%, $p < 0.01$), whereas for transitional cell metaplasia no difference was observed (Fig. 3f–g).

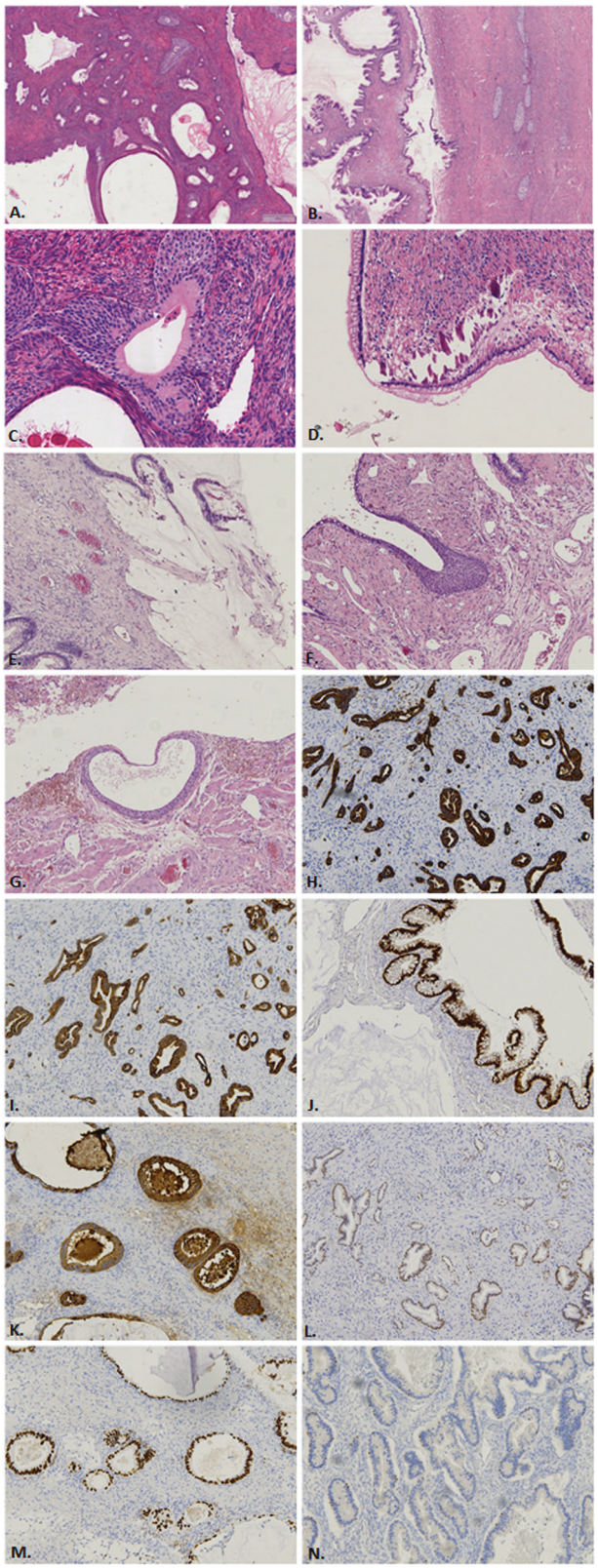

Fig. 3 **a**, **b** Histology of mixed and compartmental distribution of Brenner tumor and mucinous components. **c** Mucinous metaplasia in Brenner tumor. **d** Calcifications. **e** Mucinous stromal dissection. **f** Transitional cell metaplasia. **g** Walthard cells nests. **h–n** Protein expression of CK7, CK20, CDx2, CEA, HNF4α, SATB2 and PAX8, respectively

Protein expression in Brenner tumor-associated and teratoma-associated mucinous tumors

Thirty-eight Brenner tumor-associated mucinous tumors (17 cystadenomas, 17 atypical proliferative tumors, and 4 carcinomas) and 27 teratoma-associated mucinous tumors (12 cystadenomas, 11 atypical proliferative tumors and 4 carcinomas) were randomly selected for immunohistochemical analyses (Figs. 2c, 3h–n). Brenner tumor-associated mucinous tumors were significantly more often positive for CK7 ($p = 0.02$) and negative for both CDx2 ($p = 0.04$), MUC4 ($p = 0.02$) and SATB2 ($p < 0.01$). Associated Brenner tumors showed comparable patterns. No differences were observed between Brenner tumor-associated and teratoma-associated mucinous tumors for gastrointestinal markers such as CK20, HNF4α, and CEA-m and gynecological markers such as OC-125, ER, PR, PAX8, and WT1.

For carcinomas only, there were no statistical differences, although all Brenner tumor-associated carcinomas were negative for SATB2. Mismatch repair proteins were expressed in all carcinomas. Her2/neu status and *MYC* amplification was not different between Brenner tumor-associated and teratoma-associated mucinous tumors.

Expression of CK20, CDx2, CEA-m and HNF4α increased significantly when Brenner tumor-associated mucinous tumors progressed (cystadenoma—atypical proliferative tumor—carcinoma) ($p < 0.01$, $p < 0.01$, $p = 0.02$ and $p = 0.03$, respectively), whereas CK7 expression decreased in this group ($p < 0.01$). Teratoma-associated mucinous tumors showed a comparable trend without reaching statistical significance.

One Brenner tumor-associated carcinoma and one teratoma-associated atypical proliferative tumor were positive for Her2/neu. No *MYC* amplification was noted in any tumor. See Table S3.

Copy number analysis in Brenner tumor-associated and teratoma-associated mucinous tumors

Copy number analysis was performed for 24 Brenner tumor-associated and 22 teratoma-associated mucinous tumor pairs that were randomly selected. Twelve random normal samples (6 from Brenner tumor-associated and 6 from teratoma-associated mucinous tumor patients) were used for normalization of tumor profiles. Brenner tumor-associated mucinous tumors showed a mean of 7% aberrant bins compared to 19% in teratoma-associated mucinous tumors ($p = 0.04$). For carcinomas only, the mean percentage of aberrant bins was 14% for Brenner tumor-associated mucinous tumors and 34% for teratoma-associated mucinous tumors ($p = 0.24$). Brenner tumors had 3% aberrant bins compared to 2% in teratomas ($p = 0.63$). Frequency plots of copy number alterations in Brenner tumor-

associated and teratoma-associated mucinous tumors are found in Figure S1. The ten lowest *p*-values were selected/ (range 0.02–0.07). Statistically significant were alterations of 5q11.1–5q13.2 ($p = 0.02$), 5q13.2–5q13.3 ($p = 0.02$), 5q13.3 ($p = 0.04$), 5q13.3-5q35.3 ($p = 0.02$), 9p21.3a ($p = 0.03$) and 11p15.5–11q25 ($p = 0.03$). Regions 9p21.3b, 4p16.3–4q35.2, 9q22.32 and 13q11–13q34, showed trends but no statistical significance. Some of the regions concerned large parts of chromosomal arms (see Fig. S2 and Table S4). The region 9p21.3b overlaps with the genes *CDKN2A/CDKN2B*, and 9p21.3a is positioned just 100 kbp upstream. The gene *MTAP* is localized in between 9p21.3a and 9p21.3b. Although not statistically significant, deletion or loss of *CDKN2A/CDKN2B* was detected in eight Brenner tumor-associated mucinous tumors (33%), compared to only two deletions in teratoma-associated mucinous tumors (9%). These occurred only in atypical proliferative tumors and carcinomas. Co-deletion or loss of 9p.21.3a and *MTAP* was found in eight out of ten cases. Three Brenner tumors showed an identical gain of 5q13.2–5q13.3 as the associated mucinous tumor. No other identical copy number alterations were observed for the regions mentioned. Details of copy number alterations of these regions per mucinous tumor are displayed in Fig. 4a.

Based on copy number alterations, one cystadenoma and Brenner tumor were likely clonal. At first, clonality analysis showed three tumor pairs with a high likelihood of clonality (Fig. 5a). However, two cases showed 0% and around 1% copy number alterations, while one case, a Brenner tumor and cystadenoma, showed a high frequency of copy number alterations in both samples (Fig. 5b). This case also showed an identical gain of 5q13.2–5q13.3 in the Brenner tumor and the associated mucinous tumor. Normal tissue of this patient did not contain the same copy number alteration, excluding germ line variations.

Mutations in Brenner tumor-associated and teratoma-associated mucinous tumors

Single-molecule molecular inversion probe-based next generation sequencing mutation analysis was performed for 13 Brenner tumor-associated mucinous tumors and 17 teratoma-associated mucinous tumors, their associated Brenner tumor or teratoma and normal tissue. One Brenner tumor-associated mucinous tumor pair was excluded due to the low coverage. Details of coverage per target region per tumor are found in Table S5.

Mucinous tumors showed mutations in *KRAS* (37%), *TP53* (17%), *RNF43* (13%), *ELF3* (10%), *GNAS* (7%), *CDKN2A* (7%), *BRAF* (3%), *PIK3CA* (3%), *ERBB2* (3%) and *ACVR1B* (3%). *KRAS*, *TP53*, *CDKN2A* and *ELF3* mutations were observed in both Brenner tumor-associated (31%, 15%, 8% and 15%) and teratoma-associated mucinous tumors (41%, 18%, 6%, and 6%). *KRAS* and *TP53* mutations were found in cystadenomas, atypical proliferative tumors and carcinomas. *BRAF* and *PIK3CA* mutations occurred only in Brenner tumor-associated mucinous tumors (both 8%) and mutations in *RNF43*,

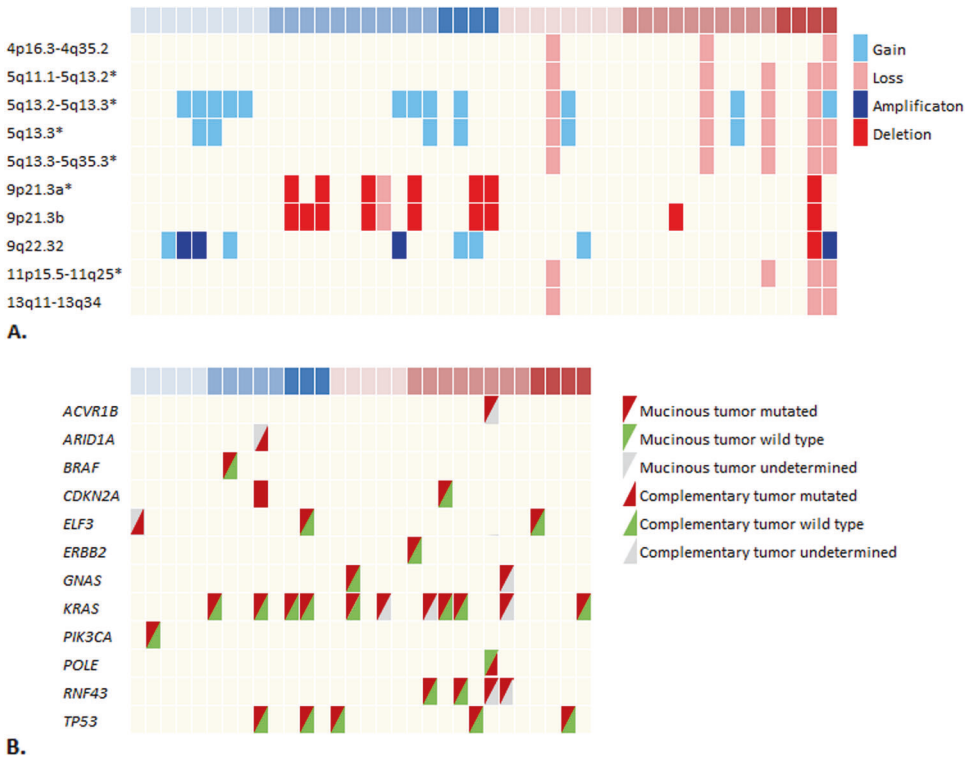

Fig. 4 Copy number alterations and mutations specifically depicted per tumor. **a** The heatmap showing amplifications, deletions, copy number gains and losses in Brenner tumor-associated and teratoma-associated mucinous tumors. Regions 9p21.3a and b coincide with *MTAP* and *CDKN2A/CDKN2B*. *$p < 0.05$. **b** The heatmap showing mutations per gene for Brenner tumor-associated and teratoma-associated mucinous tumors. Brenner tumor-associated mucinous tumors are indicated in blue, teratoma-associated mucinous tumors in red from light to dark for cystadenomas, atypical proliferative mucinous (borderline) tumors and carcinomas, respectively

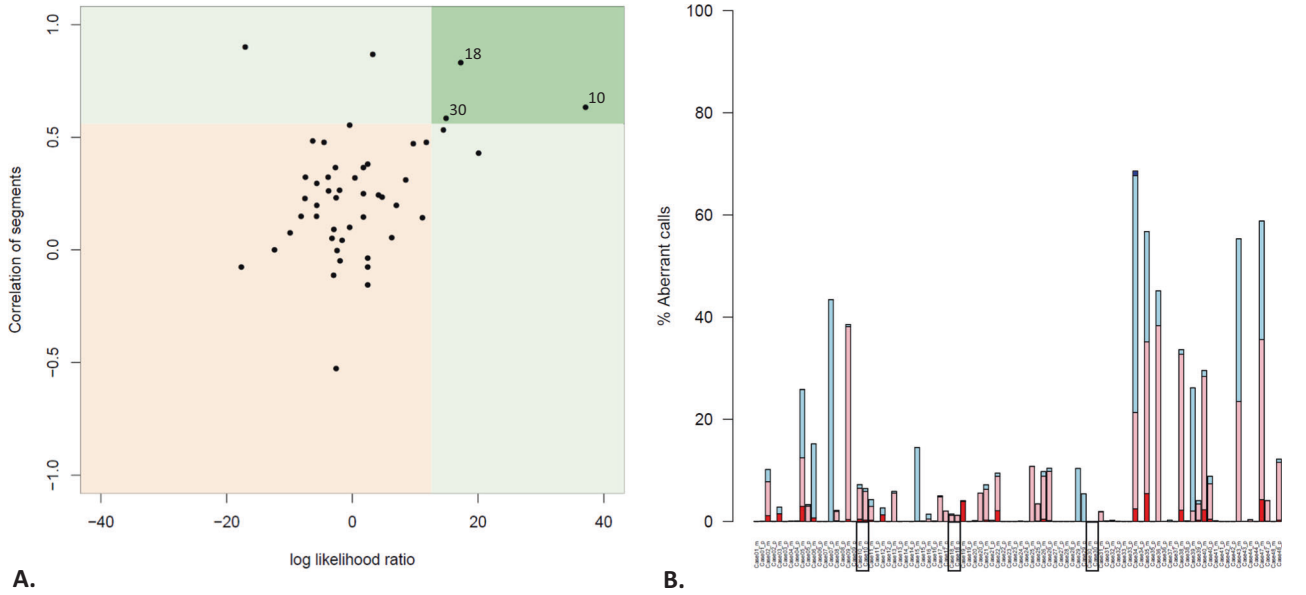

Fig. 5 **a** Scatter plot showing likelihood of clonality based on copy number analysis. The *x*-axis shows the Pearson's correlation, the *y*-axis shows clonality analysis based on copy number alterations of chromosomal arms. Thresholds were set at 90% of the data. The three cases appearing in the upper right dark green square have a high likelihood of clonality. **b** The percentage of copy number alterations per tumor pair in numerical order (mucinous tumor followed by precursor), with the clonally related cases highlighted by rectangular boxes. The percentage of copy number alterations in case 30 is 0.0%

GNAS, *ERBB2* and *ACVR1B* occurred only in teratoma-associated mucinous tumors (24%, 12%, 6%, and 6%, respectively). *RNF43* mutations did not occur in cystadenomas. One atypical proliferative mucinous tumor and associated Brenner tumor showed an identical deletion in *CDKN2A* that was not present in normal tissue. Mutations per mucinous tumor are depicted in Fig. 4b. Details on mutations per gene per tumor are found in Table S6.

In the two tumors containing *CDKN2A* mutations we further investigated the presence of loss of heterozygosity (LOH). In case 12, the variant allele frequency of *CDKN2A* was 51% with an estimated tumor cell percentage of 40%. This meant that the tumor cell percentage per definition represents an underestimation making it probable that no or very few tumor cells contained a wild type *CDKN2A* allele, although this was not confirmed with copy number analysis. In case 32, the variant allele frequency was 24% with a tumor cell percentage of 30%. In a nearby region one informative SNP was found with a variant allele frequency of 34% in the tumor sample and 54% in the normal tissue. In case of a tumor cell percentage of 30%, this indicates LOH of *CDKN2A*. In this case, loss of *CDKN2A* was also confirmed with copy number analysis.

Discussion

In this study we collected a large cohort of Brenner tumor-associated and teratoma-associated mucinous tumors and their associated Brenner tumor and teratoma, respectively. For two Brenner tumor-associated mucinous tumor pairs we could substantiate a clonal relationship. Several remarkable differences between Brenner tumor-associated and teratoma-associated mucinous tumors were that Brenner tumor-associated mucinous tumors frequently showed loss of *CDKN2A* and *MTAP*. In contrast, patients with teratoma-associated mucinous tumors were significantly younger and their tumors expressed SATB2 and showed mutations in *RNF43*. These findings support the thought that mucinous tumors of the ovary can originate from both Brenner tumors and teratomas, and that these are distinct entities.

Clonality analysis of 46 tumor pairs based on the copy number analysis showed three pairs of both Brenner tumor-associated and teratoma-associated mucinous tumors which were likely clonal. However, since two of these patterns showed the virtually complete absence of copy number alterations, these calls are probably false positive, resulting in only one case of copy number alteration-based clonality. With mutation analysis, we found one identical deletion in *CDKN2A* in a Brenner tumor and its associated atypical proliferative mucinous (borderline) tumor. Although deletions in this genomic region have been reported before, the absence of this specific deletion in COSMIC suggests it is uncommon and therefore a strong indication for a clonal relationship. Clonality between Brenner tumor-associated and teratoma-associated mucinous tumors and their precursor lesions has been suggested earlier using repetitive DNA sequences [6, 13–15]. Our findings further support an

origin of primary mucinous ovarian tumors in either Brenner tumors or teratomas. The fact that we could confirm the clonal relationship in only two tumors pairs, may be explained by the limited information obtained by our assays due to the relatively low number of copy number alterations in mucinous ovarian carcinomas, especially compared to highly genetically unstable carcinomas such as high-grade serous carcinomas [29–31]. The included Brenner tumors and teratomas also contained very few copy number alterations, meaning that during (pre)malignant transformation tumors become more genetically unstable, developing a more complex copy number profile than their original precursor and thus showing fewer similarities. In short, copy number analysis seems suboptimal for clonality analysis. For mutation analysis, low coverage may have impeded detection of (identical) variants. DNA quality may have influenced our results since we used formalin-fixed paraffin embedded material, sometimes over 15 years old. However, by using single unique molecule identifiers and targeting both strands for next generation sequencing the accuracy increased and formalin induced artifacts could be recognized [22]. Especially for cystadenomas, the amount of tumor cells in a selected slide may be low and difficult to macrodissect manually. Also, the specific subclones in the Brenner tumors and teratomas from which the mucinous component arose may be completely overgrown. Furthermore, we cannot certainly exclude collision tumors with another origin than assumed. However, this is unlikely since the combination of mucinous tumors with Brenner tumors and teratomas is rare.

We found changes that were shared between Brenner tumor-associated and teratoma-associated mucinous tumors. Firstly, frequently mutated genes in both tumors were *KRAS* and *TP53*, occurring in cystadenomas, atypical proliferative tumors and carcinomas. *KRAS* encodes a GTPase protein in the tyrosine kinase induced *RAS-RAF-MEK-ERK* pathway leading to cell growth, proliferation and survival and is frequently mutated in colorectal cancer [32]. Mucinous cystadenomas, atypical proliferative mucinous tumors and mucinous carcinomas of the ovary have been shown to frequently contain *KRAS* mutations [16, 17, 33, 34]. This seems to be an early event in tumorigenesis, where the lack of *KRAS* mutations in precursor Brenner tumors and teratomas suggests a role in development of mucinous phenotype. We found *TP53* mutations in cystadenomas, atypical proliferative tumors and carcinomas, consistent with earlier studies [16, 17, 33, 34]. *TP53* mutations, which are mainly associated with high-grade serous carcinomas and serve as a hallmark for type II ovarian carcinomas, are generally associated with poor prognosis. These findings suggest that mutations in *TP*53 are indicative of biological behavior of tumors rather than a feature of specific tumor types and that the assumption of mucinous ovarian carcinomas being solely type I carcinomas is unjust. Although mucinous ovarian carcinomas are generally regarded low grade, indolent tumors, a minority presents as advanced stage disease with extremely poor prognosis [1]. It is possible that the origin of the carcinoma is the underlying cause of this prognostic difference, but this remains to be investigated.

Secondly, Brenner tumor-associated and teratoma-associated mucinous tumors both show a gastrointestinal immunophenotype during transformation towards malignancy. Brenner tumor -associated mucinous tumors showed no expression of typical Müllerian markers such as PAX8 as reported before [3, 10, 12]. This further supports that Brenner tumor-associated and teratoma-associated mucinous tumors follow a comparable carcinogenetic pathway culminating in carcinoma, which is characterized by a gastrointestinal mucinous phenotype. This might offer new possibilities for tailored treatment for this subgroup, along the lines of systemic treatment for colorectal cancer.

Interestingly, there also were remarkable differences between Brenner tumor-associated and teratoma-associated mucinous tumors. Patients with teratoma-associated mucinous tumors were significantly younger than patients with Brenner tumor-associated mucinous tumors and patients with serous, clear cell, and endometrioid adenocarcinomas. There is a bias comparing age data with other carcinoma subtypes, since the majority of teratoma-associated mucinous tumors are premalignant. However, the same holds true for Brenner tumor-associated mucinous tumors, therefore the age difference between Brenner tumor-associated and teratoma-associated mucinous tumors is not affected by this bias. The age difference between Brenner tumor-associated and teratoma-associated mucinous tumors is only present in the premalignant stages, while carcinomas (albeit small in number) are diagnosed at a similar age.

The most striking difference in protein expression between Brenner tumor-associated and teratoma-associated mucinous tumors was SATB2 expression, being (weakly) positive in only one Brenner tumor-associated mucinous tumor and strongly expressed in almost half of teratoma-associated mucinous tumors. SATB2 is a protein involved in transcription regulation and chromatin remodeling, which is thought to be useful in the distinction of primary mucinous carcinomas and metastases of gastrointestinal origin, the latter being generally positive [35, 36]. However, our observations suggest that SATB2 is also positive in teratoma-associated mucinous tumors.

To strengthen the assumption that teratoma-associated mucinous tumors present with a gastrointestinal phenotype, we found *RNF43* mutations exclusively in teratoma-associated mucinous tumors, limited to the more advanced stages (atypical proliferative tumors and carcinomas).

RNF43 is a tumor suppressor gene negatively regulating Wnt signaling and is also frequently mutated in colorectal carcinomas [37]. Earlier studies also reported mutations in *RNF43* in atypical proliferative mucinous tumors (6–9%) and carcinomas (19–21%), but not in cystadenomas [16, 38]. The nearly exclusive occurrence of SATB2 positivity and *RNF43* mutations in teratoma-associated mucinous tumors, is an indication that these tumors more closely resemble gastrointestinal tumors than Brenner tumor-associated mucinous tumors, especially in earlier phases.

Copy number alterations deductable to specific cancer related genes were limited, but remarkable was deletion of 9p21 mainly in Brenner tumor-associated mucinous tumors, and exclusively in atypical proliferative tumors and carcinomas. This region contains *CDKN2A*/*CDKN2B* and *MTAP*, and is frequently deleted in a multitude of tumors. *CDKN2A* and *CDKN2B* code for the $p16^{INK4A}$ and $p14^{ARF}$, and the $p15^{INK4B}$ proteins respectively, which have tumor suppressive properties involved in cell cycle regulation. Genetic imbalance of chromosome 9p encompassing *CDKN2A* has been more often detected in mucinous cystadenomas (60%), atypical proliferative mucinous tumors (77%) and mucinous carcinomas (67–75%) [29, 34, 39]. Another study found LOH and homozygous deletions of *CDKN2A* in 55%, 59%, and 52% of mucinous cystadenomas, atypical proliferative mucinous tumors and mucinous carcinomas, respectively [16]. We found co-deletion or -loss of *MTAP* in 80% of cases, which is described in various premalignancies and cancer types in which it also predicts poor outcome [40–42]. *MTAP* codes for a key enzyme in polyamine salvage metabolism. This gene may act as a tumor suppressor, independent of *CDKN2A* alterations and directly related to its enzymatic activity [43]. Deletion of this gene offers possibilities for targeted therapies attaining purine deprivation or inhibition of purine synthesis [44].

In daily practice, the majority of mucinous ovarian carcinomas will present without an evident precursor. Part of these tumors will concern Brenner tumor-associated and teratoma-associated mucinous carcinomas. In the latter case, characterized by SATB2 expression and mucinous stromal dissection, there is a difficult differential diagnosis with metastatic colorectal carcinomas. In addition, a number of mucinous ovarian carcinomas is PAX8 positive [45, 46], whereas in our study cohort, PAX8 expression was practically absent. This suggests that there might be a yet unclarified pathway leading to development of PAX8 positive mucinous ovarian carcinomas. Validation of the described features on mucinous carcinomas without precursors is needed to further unravel different carcinogenetic pathways, determine necessary pathological workup and examine clinical implications of different subtypes of mucinous ovarian carcinomas.

Concluding, we further substantiated that at least part of primary mucinous ovarian carcinomas originates from Brenner tumors or teratomas. Our data suggest that in both Brenner tumors and teratomas early events such as *KRAS* mutations are responsible for acquisition of a mucinous phenotype. Subsequently, Brenner tumor-associated and teratoma-associated mucinous tumors follow a comparable carcinogenetic pathway to carcinoma, as shown by closing of the age gap and acquisition of a gastrointestinal immunophenotype. However, specific molecular changes in these pathways, such as deletion or loss of *CDKN2A*/*CDKN2B* and *MTAP* mainly in Brenner tumor-associated mucinous tumors and SATB2 expression and *RNF43* mutations nearly exclusively in teratoma-associated mucinous tumors support that Brenner tumor-associated mucinous tumors and teratoma-associated mucinous tumors remain entities with specific characteristics, with teratoma-associated mucinous tumors resembling gastrointestinal tumors most closely. Although we did not include survival or therapy related data, it is worth consideration that either teratoma-associated mucinous tumors or Brenner tumor-associated mucinous tumors might develop into mucinous ovarian carcinomas associated with poor prognosis, more often presenting in advanced stage. Also, specific molecular changes such as *KRAS* mutation, *ERBB2* amplification and deletion of *MTAP* may have implications for future options for targeted therapy.

Acknowledgements We thank the following pathology laboratories for supplying material: Department of Pathology, OLVG Hospital, Amsterdam (Hans Blaauwgeers, MD), Department of Pathology, Jeroen Bosch Hospital, 's-Hertogenbosch (Carolien Bronkhorst, MD), Department of Pathology, Rijnstate Hospital, Arnhem (Jos W. Meijer, MD, PhD), Department of Pathology, Elisabeth-TweeSteden Hospital, Tilburg (Anneke A. van der Wurff, MD, PhD), Laboratory for Pathology East Netherlands, Hengelo, Department of Pathology, PAMM, Eindhoven. We thank Robbert Weren, PhD and Arjen R. Mensenkamp, PhD of the Department of Human Genetics, Radboud university medical center, Nijmegen for development of the smMIP based Next Generation Sequencing panel and valuable advice regarding variant calling and analysis. We thank Jos B. Poell of the Department of Pathology, VU University Medical Center, for assistance with copy number analysis. This project was funded by the Dutch Cancer Society (project number KUN 2014-6613).

Compliance with ethical standards

Conflict of interest The authors declare that they have no conflicts of interest.

Publisher's note Springer Nature remains neutral with regard to jurisdictional claims in published maps and institutional affiliations.

References

1. Simons M, Massuger L, Bruls J, Bulten J, Teerenstra S, Nagtegaal I. Relatively poor survival of mucinous ovarian carcinoma in

advanced stage: a systematic review and meta-analysis. Int J Gynecol Cancer. 2017;27:651–8.
2. Kurman RJ, Shih IeM. The dualistic model of ovarian carcinogenesis: revisited, revised, and expanded. Am J Pathol. 2016;186:733–47.
3. Roma AA, Masand RP. Different staining patterns of ovarian Brenner tumor and the associated mucinous tumor. Ann Diagn Pathol. 2015;19:29–32.
4. Seidman JD, Khedmati F. Exploring the histogenesis of ovarian mucinous and transitional cell (Brenner) neoplasms and their relationship with Walthard cell nests: a study of 120 tumors. Arch Pathol Lab Med. 2008;132:1753–60.
5. Kondi-Pafiti A, Kairi-Vassilatou E, Iavazzo C, Vouza E, Mavrigiannaki P, Kleanthis C, et al. Clinicopathological features and immunoprofile of 30 cases of Brenner ovarian tumors. Arch Gynecol Obstet. 2012;285:1699–702.
6. Wang Y, Wu RC, Shwartz LE, Haley L, Lin MT, Shih IeM, et al. Clonality analysis of combined Brenner and mucinous tumours of the ovary reveals their monoclonal origin. J Pathol. 2015;237:146–51.
7. Tafe LJ, Muller KE, Ananda G, Mitchell T, Spotlow V, Patterson SE, et al. Molecular genetic analysis of ovarian brenner tumors and associated mucinous epithelial neoplasms: high variant concordance and identification of mutually exclusive RAS driver mutations and MYC amplification. Am J Pathol. 2016;186:671–7.
8. Deka R, Chakravarti A, Surti U, Hauselman E, Reefer J, Majumder PP, et al. Genetics and biology of human ovarian teratomas. II. Molecular analysis of origin of nondisjunction and gene-centromere mapping of chromosome I markers. Am J Hum Genet. 1990;47:644–55.
9. Surti U, Hoffner L, Chakravarti A, Ferrell RE. Genetics and biology of human ovarian teratomas. I. Cytogenetic analysis and mechanism of origin. Am J Hum Genet. 1990;47:635–43.
10. Vang R, Gown AM, Zhao C, Barry TS, Isacson C, Richardson MS, et al. Ovarian mucinous tumors associated with mature cystic teratomas: morphologic and immunohistochemical analysis identifies a subset of potential teratomatous origin that shares features of lower gastrointestinal tract mucinous tumors more commonly encountered as secondary tumors in the ovary. Am J Surg Pathol. 2007;31:854–69.
11. Ronnett BM, Seidman JD. Mucinous tumors arising in ovarian mature cystic teratomas: relationship to the clinical syndrome of pseudomyxoma peritonei. Am J Surg Pathol. 2003;27:650–7.
12. McKenney JK, Soslow RA, Longacre TA. Ovarian mature teratomas with mucinous epithelial neoplasms: morphologic heterogeneity and association with pseudomyxoma peritonei. Am J Surg Pathol. 2008;32:645–55.
13. Kerr SE, Flotte AB, McFalls MJ, Vrana JA, Halling KC, Bell DA. Matching maternal isodisomy in mucinous carcinomas and associated ovarian teratomas provides evidence of germ cell derivation for some mucinous ovarian tumors. Am J Surg Pathol. 2013;37:1229–35.
14. Fujii K, Yamashita Y, Yamamoto T, Takahashi K, Hashimoto K, Miyata T, et al. Ovarian mucinous tumors arising from mature cystic teratomas-a molecular genetic approach for understanding the cellular origin. Hum Pathol. 2014;45:717–24.
15. Snir OL, Buza N, Hui P. Mucinous epithelial tumours arising from ovarian mature teratomas: a tissue genotyping study. Histopathology. 2016;69:383–92.
16. Ryland GL, Hunter SM, Doyle MA, Caramia F, Li J, Rowley SM, et al. Mutational landscape of mucinous ovarian carcinoma and its neoplastic precursors. Genome Med. 2015;7:87.
17. Mackenzie R, Kommoss S, Winterhoff BJ, Kipp BR, Garcia JJ, Voss J, et al. Targeted deep sequencing of mucinous ovarian tumors reveals multiple overlapping RAS-pathway activating mutations in borderline and cancerous neoplasms. BMC Cancer. 2015;15:415.
18. Casparie M, Tiebosch AT, Burger G, Blauwgeers H, van de Pol A, van Krieken JH, et al. Pathology databanking and biobanking in The Netherlands, a central role for PALGA, the nationwide histopathology and cytopathology data network and archive. Cell Oncol. 2007;29:19–24.
19. Wolff AC, Hammond ME, Hicks DG, Dowsett M, McShane LM, Allison KH, et al. Recommendations for human epidermal growth factor receptor 2 testing in breast cancer: American Society of Clinical Oncology/College of American Pathologists clinical practice guideline update. J Clin Oncol. 2013;31:3997–4013.
20. Scheinin I, Sie D, Bengtsson H, van de Wiel MA, Olshen AB, van Thuijl HF, et al. DNA copy number analysis of fresh and formalin-fixed specimens by shallow whole-genome sequencing with identification and exclusion of problematic regions in the genome assembly. Genome Res. 2014;24:2022–32.
21. van de Wiel MA, Brosens R, Eilers PH, Kumps C, Meijer GA, Menten B, et al. Smoothing waves in array CGH tumor profiles. Bioinformatics. 2009;25:1099–104.
22. Eijkelenboom A, Kamping EJ, Kastner-van Raaij AW, Hendriks-Cornelissen SJ, Neveling K, Kuiper RP, et al. Reliable next-generation sequencing of formalin-fixed, paraffin-embedded tissue using single molecule tags. J Mol Diagn. 2016;18:851–63.
23. O'Roak BJ, Vives L, Fu W, Egertson JD, Stanaway IB, Phelps IG, et al. Multiplex targeted sequencing identifies recurrently mutated genes in autism spectrum disorders. Science. 2012;338:1619–22.
24. Lek M, Karczewski KJ, Minikel EV, Samocha KE, Banks E, Fennell T, et al. Analysis of protein-coding genetic variation in 60,706 humans. Nature. 2016;536:285.
25. Ostrovnaya I, Olshen AB, Seshan VE, Orlow I, Albertson DG, Begg CB. A metastasis or a second independent cancer? Evaluating the clonal origin of tumors using array copy number data. Stat Med. 2010;29:1608–21.
26. Olshen AB, Venkatraman ES, Lucito R, Wigler M. Circular binary segmentation for the analysis of array-based DNA copy number data. Biostatistics. 2004;5:557–72.
27. van de Wiel MA, Kim KI, Vosse SJ, van Wieringen WN, Wilting SM, Ylstra B. CGHcall: calling aberrations for array CGH tumor profiles. Bioinformatics. 2007;23:892–4.
28. van de Wiel MA, Wieringen WN. CGHregions: dimension reduction for array CGH data with minimal information loss. Cancer Inf. 2007;3:55–63.
29. Gorringe KL, Jacobs S, Thompson ER, Sridhar A, Qiu W, Choong DY, et al. High-resolution single nucleotide polymorphism array analysis of epithelial ovarian cancer reveals numerous microdeletions and amplifications. Clin Cancer Res. 2007;13:4731–9.
30. Haverty PM, Hon LS, Kaminker JS, Chant J, Zhang Z. High-resolution analysis of copy number alterations and associated expression changes in ovarian tumors. BMC Med Genomics. 2009;2:21.
31. Huang RY, Chen GB, Matsumura N, Lai HC, Mori S, Li J, et al. Histotype-specific copy-number alterations in ovarian cancer. BMC Med Genomics. 2012;5:47.
32. Cancer Genome Atlas N. Comprehensive molecular characterization of human colon and rectal cancer. Nature. 2012;487:330–7.
33. Rechsteiner M, Zimmermann AK, Wild PJ, Caduff R, von Teichman A, Fink D, et al. TP53 mutations are common in all subtypes of epithelial ovarian cancer and occur concomitantly with KRAS mutations in the mucinous type. Exp Mol Pathol. 2013;95:235–41.
34. Hunter SM, Gorringe KL, Christie M, Rowley SM, Bowtell DD, Australian Ovarian Cancer Study G, et al. Pre-invasive ovarian

mucinous tumors are characterized by CDKN2A and RAS pathway aberrations. Clin Cancer Res. 2012;18:5267–77.
35. Perez Montiel D, Arispe Angulo K, Cantu-de Leon D, Bornstein Quevedo L, Chanona Vilchis J, Herrera Montalvo L. The value of SATB2 in the differential diagnosis of intestinal-type mucinous tumors of the ovary: primary vs metastatic. Ann Diagn Pathol. 2015;19:249–52.
36. Moh M, Krings G, Ates D, Aysal A, Kim GE, Rabban JT. SATB2 expression distinguishes ovarian metastases of colorectal and appendiceal origin from primary ovarian tumors of mucinous or endometrioid type. Am J Surg Pathol. 2016;40:419–32.
37. Giannakis M, Hodis E, Jasmine Mu X, Yamauchi M, Rosenbluh J, Cibulskis K. et al. RNF43 is frequently mutated in colorectal and endometrial cancers. Nat Genet. 2014;46:1264–6.
38. Ryland GL, Hunter SM, Doyle MA, Rowley SM, Christie M, Allan PE, et al. RNF43 is a tumour suppressor gene mutated in mucinous tumours of the ovary. J Pathol. 2013;229:469–76.
39. Gorringe KL, Ramakrishna M, Williams LH, Sridhar A, Boyle SE, Bearfoot JL, et al. Are there any more ovarian tumor suppressor genes? A new perspective using ultra high-resolution copy number and loss of heterozygosity analysis. Genes Chromosomes Cancer. 2009;48:931–42.
40. Powell EL, Leoni LM, Canto MI, Forastiere AA, Iocobuzio-Donahue CA, Wang JS, et al. Concordant loss of MTAP and p16/CDKN2A expression in gastroesophageal carcinogenesis: evidence of homozygous deletion in esophageal noninvasive precursor lesions and therapeutic implications. Am J Surg Pathol. 2005;29:1497–504.
41. Krasinskas AM, Bartlett DL, Cieply K, Dacic S. CDKN2A and MTAP deletions in peritoneal mesotheliomas are correlated with loss of p16 protein expression and poor survival. Mod Pathol. 2010;23:531–8.
42. Bishop DT, Demenais F, Iles MM, Harland M, Taylor JC, Corda E, et al. Genome-wide association study identifies three loci associated with melanoma risk. Nat Genet. 2009;41:920–5.
43. Christopher SA, Diegelman P, Porter CW, Kruger WD. Methylthioadenosine phosphorylase, a gene frequently codeleted with p16(cdkN2a/ARF), acts as a tumor suppressor in a breast cancer cell line. Cancer Res. 2002;62:6639–44.
44. Bertino JR, Waud WR, Parker WB, Lubin M. Targeting tumors that lack methylthioadenosine phosphorylase (MTAP) activity: current strategies. Cancer Biol Ther. 2011;11:627–32.
45. Strickland S, Wasserman JK, Giassi A, Djordjevic B, Parra-Herran C. Immunohistochemistry in the diagnosis of mucinous neoplasms involving the ovary: the added value of SATB2 and biomarker discovery through protein expression database mining. Int J Gynecol Pathol. 2016;35:191–208.
46. Chu PG, Chung L, Weiss LM, Lau SK. Determining the site of origin of mucinous adenocarcinoma: an immunohistochemical study of 175 cases. Am J Surg Pathol. 2011;35:1830–6.